Biokinetics of Hg and Pb accumulation in the encapsulated egg of the common cuttlefish Sepia officinalis: radiotracer experiments

Thomas Lacoue-Labarthe, Michel Warnau, Marc Metian, François Oberhänsli, Claude Rouleau, Paco Bustamante

Biokinetics of Hg and Pb accumulation in the encapsulated egg of the common cuttlefish *Sepia officinalis*: radiotracer experiments

Lacoue-Labarthe T.[1*], Warnau M.[2†], Metian M.[1,2], Oberhänsli F.[2], Rouleau C.[3], Bustamante P.[1]

1- Littoral, Environnement et Sociétés (LIENSs), UMR 6250, CNRS-Université de La Rochelle, 2 rue Olympe de Gouges, F-17042 La Rochelle Cedex 01, France

2- International Atomic Energy Agency – Marine Environment Laboratories, 4 Quai Antoine Ier, MC-98000 Principality of Monaco

3- Institut Maurice-Lamontagne, 850 Route de la Mer, C.P. 1000, Mont-Joli, Québec, Canada

Correspondance to: Dr. Paco Bustamante
LIENSs, UMR 6250, CNRS-Université de La Rochelle
2 rue Olympe de Gouges
F-17042 La Rochelle Cedex 01 (France)
Phone: +33-546-507-625
Fax: +33-546-458-264
E-mail: pbustama@univ-lr.fr

[†]Present address: LIENSs, UMR 6250, CNRS-Université de La Rochelle, 2 rue Olympe de Gouges, F-17042 La Rochelle Cedex 01 (France) ; warnaumichel@yahoo.com

* Corresponding author; tlacouel@gmail.com, present address: LOV, UMR 7093 CNRS, BP28, 06234, Villefranche-sur-mer Cedex (France)

Abstract: Uptake and depuration kinetics of dissolved ^{203}Hg and ^{210}Pb were determined during the entire embryonic development of the eggs of the cuttlefish, *Sepia officinalis* (50 d at 17°C). ^{203}Hg and ^{210}Pb were accumulated continuously by the eggs all along the development time reaching load/concentration ratio (LCR) of 467 ± 43 and 1301 ± 126 g, respectively. During the first month, most of the ^{203}Hg and ^{210}Pb remained associated with the eggshell indicating that the latter acted as an efficient shield against metal penetration. From this time onwards, ^{203}Hg accumulated in the embryo, indicating that it passed through the eggshell, whereas ^{210}Pb did not cross the chorion during the whole exposure time. It also demonstrated that translocation of Hg associated with the inner layers of the eggshell is a significant source of exposure for the embryo. This study highlighted that the maturing embryo could be subjected to the toxic effects of Hg in the coastal waters where the embryonic development is taking place.

Key Words: Cephalopod, Metals, Kinetics, Embryo, Eggshell, Permeability

Introduction:

The primarily source of Hg and Pb contamination in the marine environment is their release from anthropogenic activities in the atmosphere which constitutes the principal vector toward the Ocean (Cossa et al., 2002). Hg and Pb are also discharged in coastal waters due to the contaminated flow of the urbanized watershed. The Seine River is one of the most polluted rivers in Europe and is a source of elevated amounts of Hg (*ibid.*) and Pb (Chiffoleau et al., 1994) that are released in the English Channel. The Bay of Seine (Normandy, France) into which the Seine River flows is therefore an interesting system to study Hg and Pb coastal contamination (Chiffoleau et al., 1994; Metian et al., 2008).

In the English Channel, the common cuttlefish *Sepia officinalis* lives offshore during the winter season and makes long reproductive migrations in spring to mate and to spawn in the coastal waters where they eventually die (Boucaud-Camou and Boismery, 1991). The eggs laid in the coastal shallow waters are thus subjected to acute and/or chronic exposure to various contaminants, such as metals, originating from land-based anthropogenic activities. As eggs are fixed on substrata, exposure to Hg and Pb may occur during the whole embryonic development as well as during the juvenile stage until the new cohort leaves the coast towards deeper waters. Both Hg and Pb are known to affect severely embryonic and larval development of marine invertebrates, Hg being more toxic than Pb (e.g. Calabrese et al., 1973; Warnau and Pagano, 1994; Warnau et al., 1996; Sanchez et al., 2005). Studies on early life stages of fish, echinoderms and crustaceans have shown that embryos protected by a chorionic egg envelope were generally less sensitive than larvae, which are directly in contact with waterborne contaminants (e.g. Van Leeuwen et al., 1985; Warnau and Pagano, 1994; Warnau et al., 1996; Lavolpe et al., 2004). Nevertheless, the protective role of the envelope seems to be specific for the considered metal. For example, the embryo of the steelhead trout (*Salmo gairdneri*) was shown to be more resistant to Cd, Pb, and Zn but significantly less

resistant to Ag, Cu and Hg when the egg capsule was removed than with the capsule intact (Rombough, 1985). The latter observations indicated that the presence of the egg envelope was enhancing the bioaccumulation of the first elements in the *S. gairdneri* embryo, whereas it hampered the entry of the others. In the cuttlefish, the retention/diffusion properties of the egg envelope vary throughout the development as the latter one evolves to supply the needs of the embryo in terms of space and metabolic requirements, i.e. it becomes permeable to water and gases (Gomi et al., 1986; Cronin and Seymour, 2000). In this respect, the egg of the medaka *Oryzias latipes* accumulates more Cd before the water hardening of the chorion (Gonzalez-Doncel et al., 2003) whereas the egg of the chladocera *Daphnia magna* is more sensitive to the same metal at its last embryonic stages (Bodar et al., 1989).

As many cephalopods, cuttlefish lay eggs encapsulated by three envelopes (Boletzky, 1986): the telolecithe oocyte is first surrounded by a first membrane (i.e. the chorion) derived from the follicular cells in the ovary; at spawning time, the oocyte is then embedded by mucosubstances produced by the oviductal gland; finally, once released in the mantle cavity, the oocyte is enwrapped by several layers of nidamental gland secretions stained with ink (Jecklin, 1934; Zatylny et al., 2000) (Fig. 1). These different layers protect the embryo against the surrounding environment, e.g. microbial infection and predation (Boletzky, 1986). During the embryonic development, the eggshell first hardens and becomes thicker because of the polymerization of its components (Fig. 2). This reaction leads to 1) a loss of the water contained in the mucopolysaccharidic components and 2) a decrease in egg weight. Afterwards, the egg slowly grows until the end of the organogenesis (Fig. 2). From this time onward, the egg weight increases rapidly due to the entry of water which is incorporated into the peri-vitelline fluid in order to allow sufficient space for the embryo to grow. Along these morphological changes, the eggshell becomes thinner, being almost transparent at the moment of hatching (Wolf et al., 1985; Gomi et al., 1986).

Cuttlefish eggshell is likely to act as a protective barrier hindering the incorporation of dissolved metals into the embryo, as suggested for various metals and radionuclides such as ^{241}Am, Cd, Co, Cs, Pb, V and Zn (Miramand et al., 2006; Bustamante et al., 2002, 2004, 2006). However, few information is available regarding the behaviour of these elements during the whole egg development nor regarding the related influence of structural and physiological changes of the egg (Lacoue-Labarthe et al., 2008).

As for Hg and Pb, very little is documented, despite the fact that the penetration of these highly toxic metals could lead to severe disturbance of the embryogenesis. To the best of our knowledge, only one study investigated toxic consequences in cuttlefish embryos following an acute exposure of the eggs to very high concentrations of Hg, i.e. 10 ppm (D'Aniello et al., 1990).

In this context, the aim of this study was to investigate the behaviour of Hg and Pb towards cuttlefish eggs chronically exposed to the metals dissolved in seawater, from spawning time to hatching. Gamma-emitting radiotracers, ^{203}Hg and ^{210}Pb, were used to describe the bioaccumulation (uptake and loss kinetics) of both metals at low (background) exposure concentrations. The distribution of the metals among the eggshell, the vitellus, the embryo and the peri-vitelline fluid was assessed in order to determine the changes in the eggshell permeability and subsequent bioaccumulation according to the development stages. Autoradiography was also used to locate the radiotracers in the egg compartment.

Materials and methods

1. Organisms, radiotracers and experimental procedure

Adult cuttlefish were collected by net-fishing off Monaco in March and April 2006. They were acclimated and maintained in open-circuit 600-l tanks in the IAEA-MEL premises. After mating, the fertilized eggs laid by the females were immediately separated to optimise their

oxygenation and used for the experiments. Each of two batches of eggs (n = 310 each), originating from two different females, were placed separately for up to 50 d in 20-l glass aquaria containing natural filtered - 0.45 µm- seawater (constantly aerated closed circuit; temperature 17 ± 0.5°C; 37 p.s.u.; light/dark cycle 12h/12h) spiked with ^{203}Hg (0.5 kBq l^{-1}) and ^{210}Pb (0.5 kBq l^{-1}), respectively. In terms of stable metal addition, these activity concentrations corresponded to 9 ng Hg l^{-1} and 512 µg Pb l^{-1}.

Radiotracers, ^{203}Hg [as $^{203}HgNO_3$; $t_{1/2}$ = 47 d] and ^{210}Pb [as $^{210}Pb(NO_3)_2$; $t_{1/2}$ = 22 y] were purchased from Isotope Product Laboratory, USA and from CERCA LEA, France, respectively. Stock solutions were prepared in 1 and 3 N nitric acid for ^{203}Hg and ^{210}Pb, respectively, to obtain radioactivities allowing the use of spikes of only a few microliters (typically 5 µl).

Radiotracer spikes and seawater were renewed daily during the first week and then every second day to maintain water quality and radiotracer concentrations constant. Radiotracer activities in seawater were checked before and after each water renewal in order to determine the time-integrated radiotracer activities (Rodriguez y Baena et al., 2006). At different time intervals, radiotracer activities were counted in the same tag-identified eggs (n = 8) all along the experiment. In addition, at each counting time, 4 additional eggs were counted and dissected to determine the radiotracer distribution between the eggshell and the vitellus. After one month of development, embryo and peri-vitelline fluid reached a sufficient size to be distinguished, and were then separated and counted at each sampling time.

After 7, 18, 27, and 40 days of exposure, part of the eggs (n = 70, 60, 50, 40, respectively) were removed from the exposure aquarium and held in non-exposure conditions in a 70-l glass aquarium supplied with clean flowing seawater (open circuit with constant aeration; seawater flux 50 l h^{-1}; temperature 17 ± 0.5°C; 37 p.s.u.; light/dark cycle 12h/12h). At different time intervals during the non-exposure period, the same tag-identified eggs (n = 8)

were γ-counted to establish the depuration kinetics of the radiotracers. At the end of the depuration period, the radiotracer distribution among the different egg compartments was determined by dissection of 4 eggs. Additionally, 8 unexposed eggs were distinctly tagged and placed in the same aquarium to be used as control for possible ^{203}Hg and ^{210}Pb recycling via seawater. Due to technical problems, the ^{210}Pb depuration kinetics after an 18-d exposure could not be determined.

2. Radioanalysis and data treatment

The radiotracers were γ-counted using two NaI detectors connected to a multichannel analyser (Intergamma, Intertechnique). The detectors were calibrated with an appropriate standard for each sample geometry used and measurements were corrected for background and physical decay of the radiotracers. Counting times were adapted to obtain relative propagated errors less than 5%. They ranged from 10 to 30 min for whole eggs and from 10 min to 24h for the dissected compartments.

Uptake of ^{203}Hg and ^{210}Pb was expressed as change in load/concentration ratio (LCR; ratio between radiotracer content in the egg or egg compartment –Bq– and time-integrated activity in seawater –Bq g^{-1}) along time (Lacoue-Labarthe et al., 2008, 2009). Whole radioactivity content in the eggs or in the egg compartments was considered in order to take into account the variations in weight of whole eggs and egg compartments due to vitellus reduction, embryo growth and incorporation of water during the development (Lacoue-Labarthe et al., 2008).

Uptake kinetics were best described by either a linear equation (Eq. 1), an exponential + linear combined equation (Eq. 2), or a logistic + exponential combined equation (Eq. 3):

$$LCR_t = k_u\, t \qquad \text{(Eq. 1)}$$

$LCR_t = LCR_{ss} (1-e^{-ke1\ t}) + k_{u2}\ t$ with $LCR_{ss} = k_{u1} / k_{e1}$ (Eq. 2)

$LCR_t = LCR_{ss}(1-e^{-ke\ t}) / (1+e^{-ke(t-I)})$ (Eq. 3)

where LCR_t and LCR_{ss} (g) are the load/concentration ratios at time t (d) and at steady-state, respectively, k_u and k_e are the biological uptake and depuration rate constants (g d^{-1}), respectively (Whicker and Schultz, 1982), « 1 » and « 2 » subscripts refer to the first and second phases of the uptake kinetics (Rouleau et al., 1998) and *I* is a constant.

Constants (and their statistics) of the best fitting equations (decision based on ANOVA tables for two fitted model objects) were estimated by iterative adjustment of the models using the *nls* curve-fitting routine in R freeware (Lacoue-Labarthe et al., 2008).

Radiotracer depuration kinetics were expressed in terms of change of percentage of remaining activity (i.e., radioactivity at time t divided by initial radioactivity measured in the egg or in the egg compartment at the beginning of the depuration period * 100) along time.

The depuration kinetics were best fitted by either a single (Eq. 4) or a double (Eq. 5) exponential equation:

$A_t = A_0\ e^{-ke\ t}$ (Eq. 4)

$A_t = A_{0s}\ e^{-kes\ t} + A_{0l}\ e^{-kel\ t}$ (Eq. 5)

where A_t and A_0 are the remaining activities (%) at time t (d) and 0, respectively, k_e is the biological depuration rate constant (d^{-1}), and « s » and « l » subscripts refer to the short- and long-lived component of the depuration kinetics (Warnau et al., 1999). The determination of k_e allows the calculation of the radiotracer biological half-life ($Tb_{1/2} = \ln 2 / k_e$).

The differences between the metal uptake capacities in the whole egg and in the eggshell were tested by the non-parametric test of Mann-Whitney (U-test).

The level of significance for statistics and modelling was always set at $\alpha < 0.05$.

3. Autoradiography

Following exposure to dissolved ^{203}Hg and ^{210}Pb for the first 15 d of their development, 5 eggs were embedded in a 2.5% carboxymethylcellulose gel and flash-frozen in a slurry of dry ice in hexane. From each egg, 20-µm thick sections were cut with a specially designed cryomicrotome (Leica CM3600). Sections were then freeze-dried and placed on phosphor screens (Perkin-Elmer) for 4 to 7 d. After exposure, the screens were scanned with a Cyclone Phosphor Imager (Perkin-Elmer) and ^{203}Hg and ^{210}Pb activities in egg compartments were quantified as previously described (Rouleau et al., 2003).

Results

1. Uptake kinetics in whole eggs and in egg compartments

^{203}Hg and ^{210}Pb were constantly taken up by the whole egg all along the development time (Fig. 3). ^{210}Pb uptake kinetic was best described by a linear equation whereas ^{203}Hg accumulation showed a two-step process (exponential + linear combined equation), with a first rapid adsorption component (k_{u1} = 59 g d^{-1}) followed by a slower uptake phase (k_{u2} = 6 g d^{-1}). Egg displayed greater accumulation efficiencies for ^{210}Pb than for ^{203}Hg, reaching LCR values of, respectively, 1301 ± 126 g and 467 ± 43 g a few hours before hatching.

Considering uptake kinetics in the two main egg compartments (i.e. eggshell and embryo; Figure 4), it is worth noting that the accumulation of both ^{203}Hg and ^{210}Pb in the eggshell displayed a similar pattern to that observed in the whole egg. Indeed, the eggshell revealed strong accumulation capacities with LCR reaching 556 ± 45 and 1390 ± 188 g for ^{203}Hg and ^{210}Pb, respectively, at the end of development. These LCR were not significantly different from those determined in the whole egg (U-test; $p = 0.239$).

In the embryo, ^{203}Hg was accumulated following a combined equation (saturation + logistic) with an estimated LCR_{ss} of 99 ± 18 g, which was not reached at day 50 (LCR_{50d} = 61 ± 1 g). In contrast, the embryo did not show any detectable ^{210}Pb accumulation with time.

The distribution of ^{203}Hg and ^{210}Pb in the different egg compartments (Table 1) confirmed that the greatest proportion of both metals remained associated with the eggshell, i.e. > 90% all along the embryo development. Nevertheless, after 33d of exposure, 2.5% of the total ^{203}Hg content in the egg was found in the embryo and 1% in the vitellus, showing that this element had actually penetrated the eggshell. The proportion of ^{203}Hg in the embryo increased during the development and the embryo contained 10% of the total body load at day 48, showing its effective accumulation in embryonic tissues. As for ^{210}Pb, it was never detected in the internal compartments, i.e. the embryo, the vitellus or the peri-vitelline fluid until the end of development. At that time, extremely low activities of ^{210}Pb (< 1.5 Bq) were found in the embryo.

2. Depuration kinetics in the whole eggs

For both metals, the depuration kinetics after 7, 27 and 40 d of exposure were fitted using a single exponential model. In contrast, a double exponential model best described the depuration kinetics after 18 d of exposure to dissolved ^{203}Hg (Table 2).

Interestingly, the retention capacity of ^{203}Hg by the eggs decreased during the development time: when the eggs were exposed during the first 7 d or during the first 48 d of their development, the biological half-life ($Tb_{½}$) of ^{203}Hg decreased from 104 to 39 d. Similarly, $Tb_{½}$ of ^{210}Pb was 1.7-fold higher following a 7-d exposure compared to that after a 27- and 40-d exposure (37 *vs.* 22 and 21 d).

The total activities (Bq) and the corresponding distribution (%) of the radiotracers among the different egg compartments at the beginning and at the end of the depuration period are presented in Table 3. The activity of ^{203}Hg increased significantly in the embryo whereas it decreased in the eggshell. After 7, 18 and 27 d of exposure, up to 2.5 % of the ^{203}Hg initially contained in the eggshell was detected in the embryo a few hours before hatching. After 40 d of exposure, no significant changes occurred in the ^{203}Hg distribution until the end of development.

3. Autoradiography

The autoradiograms of the whole egg exposed to dissolved ^{203}Hg and ^{210}Pb after 15 d of development is shown in Figure 5. Both metals were mainly associated with the outer layers of the nidamental envelope. Then, the labelling of ^{203}Hg and ^{210}Pb decreased along the inner part of the mucopolysaccharidic eggshell, suggesting a progressive diffusion in the whole thickness of the eggshell.

None of the metals was found in the internal compartments, i.e. the peri-vitelline space and the vitellus at that time of the development.

Discussion

As evoked earlier in this paper, cuttlefish egg undergoes major structural and physiological modifications during the embryonic development (Figures 1 & 2), leading to important egg weight variations. In particular, these changes provoke the dilution of the metal concentrations in the embryo and in the peri-vitelline fluid. Thus, in order to overcome these weight variations hiding metal accumulation in the eggs, the uptake of the radiotracers was expressed in terms of metallic content in the whole egg and its different compartments, i.e.

eggshell, embryo, vitellus, and peri-vitelline fluid (Lacoue-Labarthe et al, 2008).

The exposure of cuttlefish eggs to waterborne metals revealed that ^{203}Hg and ^{210}Pb were efficiently accumulated from the dissolved phase as the LCR constantly increased all along the development time (Figure 3). On the one hand, this was especially obvious for Pb, which displayed linear uptake kinetics, indicating that its accumulation was still far from reaching steady state equilibrium. On the other hand, Hg uptake was described by a two-step accumulation phase, i.e. nonlinear initial uptake followed by a slowed linear uptake. This suggests that Hg readily binds eggshell components during the first 10 d of development, and that these components have very high affinity for this metal. After this period, the slower, linear accumulation of Hg was not disturbed by the main developmental modifications of the egg (i.e. egg swelling, organogenesis, etc) until hatching time. Pb accumulation followed a similar linear uptake, all along the development period. At the end of the 50-d development, the LCR observed for Pb was 3 times higher than for Hg, suggesting that the Hg binding capacity of cuttlefish egg is rather limited. Interestingly, Hg and Pb accumulation in the eggshell followed similar kinetics (model and kinetic parameters) than in the whole egg, indicating that accumulation in cuttlefish egg was driven by the accumulation properties of the eggshell. This observation is consistent with previous studies on Hg and Pb that reported that in the egg of the common carp, *Cyprinus carpio*, more than 84% of Pb was bound on the egg chorion (Stouthart et al., 1994) and that more than 98% of Hg and Pb was associated with the collagenous eggcase of the dogfish *Scyliorhinus canicula* (Jeffree et al., 2008). In cuttlefish eggs collected from the field, Miramand et al. (2006) reported that Pb was detected only in the eggshell.

The predominant role of the eggshell in metal accumulation in cuttlefish eggs was further demonstrated by our autoradiography evidences. The latter showed that after two weeks of exposure, both Hg and Pb were mainly located on the nidamental egg envelopes (see Fig. 5).

298 The retention of both metals in the egg is therefore likely due to adsorption and/or absorption
299 on/in the eggshell layers in relation to their chemical and structural composition. In particular,
300 it is well documented that the cuttlefish eggshell is composed of sulphydryl-rich proteins and
301 carboxylic-rich mucopolysaccharides (Kimura et al., 2004) for which Hg and Pb,
302 respectively, have strong affinities (Viarengo and Nott, 1993; Gélabert et al., 2007).
303 Hg and Pb concentration in the eggshell increased throughout the embryonic life, indicating
304 that the eggshell metal-binding sites were not saturated at the end of the development time.
305 This can be due partly to the regular increase in eggshell surface after the first two weeks of
306 development as a consequence of the egg swelling, which results in a change (increase) in the
307 surface:volume ratio of the eggshell.
308 In contrast to Hg and Pb, Ag load concentration ratio in the eggshell was shown to decrease
309 with the increase of the egg weight, i.e. when the egg surface increased (Lacoue-Labarthe et
310 al., 2008), presumably because of the progressive delamination of the outer eggshell layers
311 along the embryonic development. This contrasting behaviour between Hg and Ag was
312 unexpected, since both elements have similar binding properties for sulphydryl groups
313 (Nieboer and Richardson, 1980). Such a difference strongly suggests that complex
314 mechanisms linked to the eggshell composition and structure drive the metal retention in the
315 eggshell, and stresses the need for more information on the composition and the properties of
316 the eggshell of cuttlefish eggs. Nevertheless, in the case of Hg and Pb, the eggshell would act
317 as a protective barrier limiting/hindering the incorporation of dissolved metals into the egg,
318 and, thereby, limiting exposure of the embryo.
319 These shielding properties were found to be quite efficient during the first month of
320 development: our data also clearly showed that Hg did not penetrate the eggshell during that
321 period. However, from day 30, Hg accumulated in the vitellus and in the embryo indicating
322 that the eggshell permeability changed in relation to the egg swelling process. As a result, the

323 embryo was shown to be exposed to and to accumulate Hg during the last 20 d of the
324 embryonic development period (i.e., from day 30 to 50; see Fig. 4), reaching 10% of the Hg
325 burden of the egg at the end of the development.
326 In fish eggs, Ag, Cu, and Hg were shown to be tightly bound to the capsule and to have
327 limited penetration in the egg whereas Cd, Pb, and Zn were weakly bound and could enter
328 rapidly in the peri-vitelline fluid (Rombough, 1985). Accordingly, we were expecting Pb to
329 reach the internal compartments of the cuttlefish egg more easily than Hg. This assumption
330 was not confirmed by our observations: Pb was never detected in the tissues of the embryo
331 whatever the development stage. As previously shown for other metals (e.g., Bustamante et
332 al., 2002, 2004, 2006) at low and high concentrations in seawater (Lacoue-Labarthe et al.,
333 2008), this indicates that the eggshell has a specific permeability for Hg and Pb. This may
334 arise for two reasons: (1) the eggshell binding/retention properties determine the metal
335 diffusion capacity and/or (2) the metal-selective penetration is driven by the permeability of
336 the most inner membrane, i.e. the chorion.
337 When the cuttlefish eggs were placed in depuration conditions, the retention capacity of Hg
338 and Pb decreased when pre-exposure time increased, suggesting that the binding strength of
339 metals to eggshell (i.e. the compartment driving metal accumulation in the egg) decreased
340 with the development time. Nevertheless, Hg was more strongly retained by the egg than Pb
341 ($Tb_{1/2}$: 104 *vs.* 37 d after a 7-d exposure), suggesting that the sulfhydryl-Hg binding was
342 stronger than the carboxylic-Pb binding.
343 The autoradiograms showed that both metals have a similar capacity to diffuse through the
344 different eggshell layers (see Fig. 5). Therefore, it appears that the chorionic membrane would
345 be the factor driving the selective permeability of the eggshell against Hg *vs* Pb penetration.
346 Additionally, the depuration experiments carried out after different times of metal exposure
347 demonstrated that, during the last month of the development, the Hg incorporated in the

internal compartments was at least partly originating from the translocation of the metal occurring in the eggshell towards the embryo. Indeed, during these depuration experiments, there was no other source of Hg radiotracer than the one associated with the eggshell. This process occurred after one month of development when, as previously indicated, the eggshell becomes thinner and permeable to water (Wolf et al., 1985; Cronin and Seymour, 2000). At this embryonic stage, Hg was thus able to diffuse through the nidamental and oviductal envelopes and to pass through the chorion before being accumulated in the embryo, whereas Pb always remained retained by the eggshell components.

Mechanisms leading to egg swelling in cephalopods are not completely known. Ikeda et al. (1993) showed that the oviductal mucosubstances of the eggshell trigger the formation of the peri-vitelline space in the eggs of the squid *Todarodes pacificus*. In the eggs of the cuttlefish *Sepiella japonica*, the swelling is caused by a water influx that follows an osmotic pressure sustained by the release of proteins in the peri-vitelline fluid during the development (Gomi et al., 1986). Ikeda et al. (1993) proposed that this organic material would be transferred from the inner, oviductal-originating eggshell layers to the peri-vitelline space. Provided this mechanism is similar in *S. officinalis*, Hg bound to the eggshell proteins could thus cross the chorion in association with the organic matter, and thereby reach the peri-vitelline space and become bioavailable for the embryo. In contrast, Pb could be associated with proteins that are not involved in the swelling process.

In conclusion, the cuttlefish egg showed an efficient uptake capacity for Hg and Pb. Both metals remained associated mainly with the eggshell all along the development time. Hg accumulated also in the embryo after one month of development, whereas Pb did not. This observation questioned the selective permeability of the eggshell for these two elements and the changes in its permeability according to the egg development stages. The selective metal uptake capacity appears to depend on the retention capacity of the nidamental and oviductal

envelopes and the metal diffusion property of the chorion, which are developmental stage-dependent. Further studies should be carried out in order to determine precisely the nature of the eggshell components involved in these processes and their evolution along the embryonic life. Thus, this study highlighted that the cuttlefish embryo is not completely protected against Hg exposure during the last developmental stages and that Hg accumulation during embryonic life could lead to toxic effects in the maturing embryo.

Acknowledgment: MW is an Honorary Senior Research Associate of the National Fund for Scientific Research (NFSR, Belgium) and held a 2008-2009 Invited Expert position at LIENSs (CNRS-Université de La Rochelle), supported by the Conseil Régional de Poitou-Charentes. The IAEA is grateful for the support provided to its Marine Environment Laboratories by the Government of the Principality of Monaco. This work was financially supported by the IAEA and LIENSs.

References

Bodar CWM, Zee Avd, Voogt PA, Wynne H, Zandee DI. Toxicity of heavy metals to early life stages of *Daphnia magna*. Ecotoxicol Environ Saf 1989; 17: 333-338.

Boletzky SV. Encapsulation of cephalopod embryos: a search for functional correlations. Am Malacol Bull 1986; 4: 217-27.

Boucaud-Camou E, Boismery J. The migrations of the cuttlefish (*Sepia officinalis* L) in the English Channel. In: Boucaud-Camou E, editor. The Cuttlefish. Centre de publication de l'Université de Caen, Caen, France, 1991, pp. 179-89.

Bustamante P, Teyssié J-L, Fowler SW, Cotret O, Danis B, Miramand P, Warnau M. Biokinetics of zinc and cadmium accumulation and depuration at different stages in the

398 life cycle of the cuttlefish *Sepia officinalis*. Mar Ecol Prog Ser 2002; 231: 167-77.
399 Bustamante P, Teyssié, J-L, Danis B, Fowler SW, Miramand P, Cotret O, Warnau M. Uptake,
400 transfer and distribution of silver and cobalt in tissues of the common cuttlefish *Sepia*
401 *officinalis* at different stages of its life cycle. Mar Ecol Prog Ser 2004; 269: 185-95.
402 Bustamante P, Teyssié J-L, Fowler SW, Warnau M. Contrasting bioaccumulation and
403 transport behaviour of two artificial radionuclides (^{241}Am and ^{134}Cs) in cuttlefish
404 eggshell. Vie Milieu 2006 ; 56 : 153-56.
405 Calabrese A, Collier RS, Nelson DA, MacInnes JR. The toxicity of heavy metals to embryo
406 of the american oyster *Crassostrea virginica*. Mar Biol 1973 ; 18: 162-66.
407 Chiffoleau J-F, Cossa D, Auger D, Truquet I. Trace metal distribution, partition and fluxes in
408 the Seine estuary (France) in low discharge regime. Mar Chem 1994; 47: 145-58.
409 Cossa D, Laurier FJG, Ficht A. Mercury contamination in the Seine estuary, France: an
410 overview, Chap. 20. In: Cai Y, Braids OC editors. Biogeochemistry of environmentally
411 important elements. American Chemical Society, Washington D.C., 2002, pp. 298-320.
412 Cronin ER, Seymour RS. Respiration of the eggs of the giant cuttlefish *Sepia apama*. Mar
413 Biol 2000; 136: 863-70.
414 D'Aniello A, Pischetola M, Vanacore F, De Nicola M, Denuce M. Effect of mercury,
415 cadmium and copper on the development and viability of *Loligo vulgaris* and *Sepia*
416 *officinalis* embryos. Ital J Biochem 1990; 32: 130A-2A.
417 Gélabert A, Pokrovsky OS, Schott J, Boudou A, Feurtet-Mazel A. Cadmium and lead
418 interaction with diatom surfaces: a combined thermodynamic and kinetic approach.
419 Geochim Cosmochim Acta 2007; 71: 3698-716.
420 Gomi F, Yamamoto M, Nakazawa T. Swelling of egg during development of the cuttlefish,
421 *Sepiella japonica*. Zool Sci 1986; 3: 641-45.
422 Gonzalez-Doncel M, Larrea M, Sanchez-Fortun S, Hinton DE. Influence of water hardening

423 of the chorion on cadmium accumulation in medaka (*Oryzias latipes*) eggs.
424 Chemosphere 2003; 52: 75-83.
425 Ikeda Y, Sakurai Y, Shimazaki K. Fertilizing capacity of squid (*Todarodes pacificus*)
426 spermatozoa collected from various storage sites, with special reference to the role of
427 gelatinous substance from the oviductal gland in fertilization and embryonic
428 development. Invertebr Reprod Dev 1993 ; 23, 39-44.
429 Jecklin L. Beitrag zur kenntnis der laichgallertern und der biologie der embryonen decapoder
430 cephalopoden. Rev Suisse Zool 1934; 41: 593-673.
431 Jeffree RA, Oberhansli F, Teyssié J-L. The accumulation of lead and mercury from seawater
432 and their depuration by eggs of the spotted dogfish *Scyliorhinus canicula*
433 (Chondrichthys). Arch Environ Contam Toxicol 2008; 55:451-61.
434 Kimura S, Higuchi Y, Aminaka M, Bower JR, Sakurai Y. Chemical properties of egg-mucin
435 complexes of the ommastrephid squid *Todarodes pacificus*. J Molluscan Stud 2004; 70:
436 117-21.
437 Lacoue-Labarthe T, Oberhänsli FR, Teyssié J-L, Warnau M, Koueta N, Bustamante P.
438 Differential bioaccumulation behaviour of two toxic metals (Ag and Cd) during the
439 early development of the cuttlefish *Sepia officinalis*. Aquat Toxicol 2008; 86: 437-46.
440 Lacoue-Labarthe T, Warnau M, Oberhänsli FR, Teyssié J-L, Bustamante P. Bioaccumulation
441 of inorganic Hg by the juvenile cuttlefish *Sepia officinalis* exposed to ^{203}Hg radiolabelled
442 seawater and food. Aquat Biol 2009; doi : 10.3354/ab00172.
443 Lavolpe M, Lopez Greco L, Kesselman D, Rodriguez E. Differential toxicity of copper, zinc,
444 and lead during the embryonic development of *Chasmagnathus granulatus* (Brachyura,
445 Varunidae). Environ Toxicol Chem 2004; 23: 960-67.
446 Metian M, Warnau M, Cosson R., Oberhänsli FR, Bustamante P. Bioaccumulation and
447 detoxification processes of Hg in the king scallop *Pecten maximus*: field and laboratory

448 investigations. Aquat Toxicol 2008; 90: 204-13.
449 Miramand P, Bustamante P, Bentley D, Koueta N. Variation of heavy metal concentrations
450 (Ag, Cd, Co, Cu, Fe, Pb, V, and Zn) during the life cycle of the common cuttlefish
451 *Sepia officinalis*. Sci Total Environ 2006; 361: 132-43.
452 Nieboer E, Richardson DHS. The replacement of the nondescript term 'heavy metal' by a
453 biologically and chemically significant classification of metal ions. Environm Pollut
454 1980; 1: 3-26.
455 Rodriguez-y-Baena AM, Metian M, Teyssié JL, De Broyer C, Warnau M. Experimental
456 evidence for ^{234}Th bioaccumulation in three Antarctic crustaceans: potential
457 implications in particle flux studies. Mar Chem 2006; 100: 354-65.
458 Rombough PJ. The influence of the zona radiata on the toxicities of zinc, lead, mercury,
459 copper and silver ions to embryos of steelhead trout *Salmo gairdneri*. Comp Biochem
460 Physiol 1985; 82C: 115-17.
461 Rouleau C, Block M, Tjälve H. Kinetics and body distribution of waterborne ^{65}Zn(II), ^{109}Cd(II),
462 ^{203}Hg(II), and $CH_3{}^{203}$Hg(II) in phantom midge larvae (*Chaoborus americanus*) and effects
463 of complexing agents. Environ Sci Technol 1998; 32: 1230-6.
464 Rouleau C, Xiong Z-H, Pacepavicius G, Huang G-L. Uptake of waterborne tributyltin in the
465 brain of fish : axonal transport as a proposed mechanism. Environ Sci Technol 2003;
466 37: 3298-302.
467 Sanchez MV, Cahansky AV, Lopez Greco LS, Rodriguez EM. Toxicity of mercury during
468 embryonic development of *Chasmagnathus granulatus* (Brachyura, Varunidae).
469 Environ Res 2005; 99: 72-8.
470 Stouthart AJHX, Spanings FAT, Lock RAC, Wendelaar Bonga SE. Effects of low water pH
471 on lead toxicity to early life stages of the common carp (*Cyprinus carpio*). Aquat
472 Toxicol 1994; 30: 137-51.
473 Van Leeuwen CJ, Griffioen PS, Vergouw WHA, Maas-Diepeveen JL. Differences in

susceptibility of early life stages of rainbow trout (*Salmo gairdneri*) to environmental pollutants. Aquat Toxicol 1985; 7: 59-78.

Viarengo A, Nott JA. Mechanisms of heavy metal cation homeostasis in marine invertebrates. Comp Biochem Physiol 1993; 104C: 355-72.

Warnau M, Fowler SW, Teyssié J-L. Biokinetics of radiocobalt in the asteroid *Asterias rubens* (Echinodermata): sea water and food exposures. Mar Poll Bull 1999; 39: 159-64.

Warnau M, Iaccarino M, De Biase A, Temara A. Spermiotoxicity and embryotoxicity of heavy metals in the echinoid *Paracentrotus lividus*. Environ Toxicol Chem 1996; 15: 1931-6.

Warnau M, Pagano G. Developmental toxicity of $PbCl_2$ in the echinoid *Paracentrotus lividus* (Echinodermata). Bull Environ Contam Toxicol 1994; 53: 434-41.

Whicker FW, Schultz V. Radioecology: nuclear energy and the environment. CRC Press, Boca Raton, FL, 1982.

Wolf G, Verheyen E, Vlaeminck A, Lemaire J, Decleir W. Respiration of *Sepia officinalis* during the embryonic and early juvenile life. Mar Biol 1985; 90: 35-9.

Zatylny C, Gagnon J, Boucaud-Camou E, Henry J. ILME: a waterborne pheromonal peptide released by the eggs of *Sepia officinalis*. Biochem Biophys Res Commun 2000; 275: 217-22.

Table 1. *Sepia officinalis*. Distribution (%; mean ± SD; n = 4) of ^{203}Hg and ^{210}Pb among the different cuttlefish egg compartments after 11, 33 and 48 days of exposure to the dissolved radiotracers.

	11 d		33 d		48 d	
	^{203}Hg	^{210}Pb	^{203}Hg	^{210}Pb	^{203}Hg	^{210}Pb
Eggshell	99.6 ± 0.4	99.8 ± 0.1	96.2 ± 1.2	99.7 ± 0.1	89.7 ± 1.4	99.5 ± 0.5
Vitellus	0.4 ± 0.4	< 0.1	1.0 ± 0.7	< 0.1	-	-
Embryo	-	-	2.5 ± 1.6	< 0.1	10.0 ± 1.3	0.4 ± 0.5
Peri-vitelline fluid	-	-	0.3 ± 0.04	< 0.1	0.3 ± 0.1	0.1 ± 0.1

Table 2. *Sepia officinalis*. Parameters of the equations describing the depuration kinetics of ^{203}Hg and ^{210}Pb in the whole cuttlefish eggs previously exposed to the radiotracers for (a) 7 days, (b) 18 days, (c) 27 days, or (d) 40 days. O and T: one- and two-exponential depuration equations, respectively; *** and **: p-values < 0.001 and < 0.01, respectively.

Pathway	Model	A_{0s} ± SE	k_s	$T_{b½s}$ ± SE (d)	A_{0l} ± SE	k_l	$T_{b½l}$ ± SE (d)	R^2
(a) Depuration after a 7-d exposure								
^{203}Hg	O	100 ± 1.0 ***	0.007 ***	104 ± 9***	-	-	-	0.643
^{210}Pb	O	101 ± 1.9 ***	0.019 ***	37 ± 3***	-	-	-	0.745
(b) Depuration after a 18-d exposure								
^{203}Hg	T	9.8 ± 2.5 ***	1.301	0.5 ± 0.1	90.3 ± 1.8 ***	0.009 ***	79 ± 10	0.789
^{210}Pb	O	-	-	-	-	-	-	-
(c) Depuration after a 27-d exposure								
^{203}Hg	O	101 ± 2.0 ***	0.016 ***	43 ± 6***	-	-	-	0.492
^{210}Pb	O	98.4 ± 1.4 ***	0.031 ***	22 ± 1***	-	-	-	0.886
(d) Depuration after a 40-d exposure								
^{203}Hg	O	102 ± 1.4 ***	0.018 ***	39 ± 9***	-	-	-	0.409
^{210}Pb	O	98.4 ± 0.8 ***	0.032 **	21 ± 2**	-	-	-	0.875

Table 3. *Sepia officinalis*. Activity (Bq; mean ± SD; n = 4) and distribution (%; mean ± SD; n = 4) of ^{203}Hg and ^{210}Pb in the different egg compartments at the beginning (t_0) and at the end (t_f) of the depuration period, and percentage of the activity gained or lost (+ or -) by the compartment between t_0 and t_f.

	^{203}Hg				^{210}Pb				Activity loss or gain (%)	
	t_0		t_f		t_0		t_f		^{203}Hg	^{210}Pb
	Bq	%	Bq	%	Bq	%	Bq	%		
(a) Depuration experiment after a 7-d exposure										
Eggshell	72 ± 11	99.8 ± 0.4	50 ± 25	96.5 ± 1.1	84 ± 23	99.7 ± 0.1	37 ± 11	99.7 ± 0.1	- 30	- 56
Vitellus	0.2 ± 0.2	0.2 ± 0.4	-	-	< dl	< 0.1	-	-	-	-
Embryo	-	-	1.6 ± 0.4	3.3 ± 1.1	-	-	< dl	< 0.1	+ 2.2	< 1
Peri-vitelline fluid	-	-	0.1 ± 0.03	0.2 ± 0.1	-	-	< dl	< 0.1	< 1	< 1
(b) Depuration experiment after a 18-d exposure										
Eggshell	104 ± 24	99.6 ± 0.1	72 ± 21	96.0 ± 1.0		na		na	- 31	-
Vitellus	0.4 ± 01	0.4 ± 0.1	-	-		na		na	-	-
Embryo	-	-	2.7 ± 0.2	3.7 ± 0.9		na		na	+ 2.5	-
Peri-vitelline fluid	-	-	0.2 ± 0.1	0.2 ± 0.1		na		na	< 1	-
(c) Depuration experiment after a 27-d exposure										
Eggshell	128 ± 30	98.2 ± 0.4	77 ± 8	94.0 ± 0.7	240 ± 40	99.7 ± 0.1	176 ± 28	99.3 ± 0.3	- 40	- 27
Vitellus	0.8 ± 0.1	0.6 ± 0.2	-	-	< dl	< 0.1	-	-	-	-
Embryo	1.3 ± 0.1	1.0 ± 0.3	4.6 ± 0.2	5.7 ± 0.6	< dl	< 0.1	0.9 ± 0.3	0.5 ± 0.2	+ 2.5	< 1
Peri-vitelline fluid	0.2 ± 0.03	0.1 ± 0.03	0.2 ± 01	0.3 ± 0.1	< dl	< 0.1	0.2 ± 0.2	0.1 ± 0.1	< 1	< 1
(d) Depuration experiment after a 40d exposure										
Eggshell	169 ± 10	92.7 ± 0.9	166 ± 36	91.9 ± 2.0	306 ± 98	99.7 ± 0.1	285 ± 93	99.3 ± 0.3	- 2	- 7
Vitellus	1.1 ± 0.2	0.6 ± 0.1	-	-	< dl	< 0.1	-	-	-	-
Embryo	12 ± 1.5	6.4 ± 0.8	13 ± 0.5	7.6 ± 1.6	< dl	< 0.1	1.1 ± 0.3	0.4 ± 0.2	< 1	< 1
Peri-vitelline fluid	0.5 ± 0.1	0.3 ± 0.1	0.8 ± 0.5	0.5 ± 0.4	0.2 ± 0.1	< 0.1	0.6 ± 0.4	0.2 ± 0.1	< 1	< 1

dl: detection limit; na: not available; (-) compartment absent according to the developmental stage.

Captions to figures

Fig 1. *Sepia officinalis.* Successive steps of ovulation and embedding of the eggs in the female mantle cavity. 1: full grown oocyte surrounded by the chorion; 2: oocyte with the oviductal envelope; 3: embedded oocyte with the nidamental mucosubstances and ink.
ang, accessory nidamental glands; o, ovary ; og, oviductal gland ; ot, oviductal tract ; mng, main nidamental gland (modified from Zatylny et al. 2000).

Fig 2. *Sepia officinalis*. Weight variations of the whole egg (●), the embryo (○) and the peri-vitelline fluid (PVF ; ▲) during the embryonic development and sketches of egg adapted from Gomi et al. (1986)

Fig 3. *Sepia officinalis.* Uptake kinetics of ^{203}Hg and ^{210}Pb in whole cuttlefish eggs exposed for the entire development time to the radiotracers dissolved in seawater (load-concentration ratio, LCR (g); mean ± SE, n=8)

Fig 4. *Sepia officinalis*. Uptake kinetics of ^{203}Hg and ^{210}Pb in eggshell (○) and embryo (●) of cuttlefish eggs exposed for the entire development time to the radiotracers dissolved in seawater (load-concentration ratio, LCR; mean ± SE, n=4).

Fig 5. *Sepia officinalis*. Autoradiogram of cuttlefish egg exposed to dissolved ^{203}Hg (A) and ^{210}Pb (B) during the first 15 day of development.

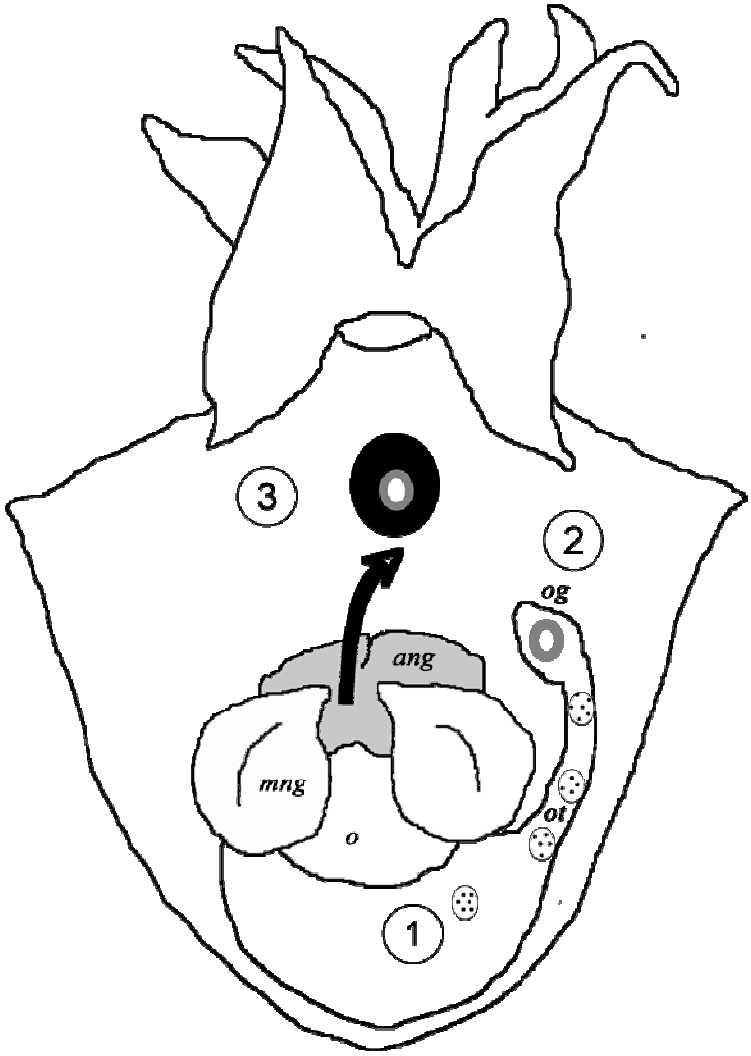

Figure 1

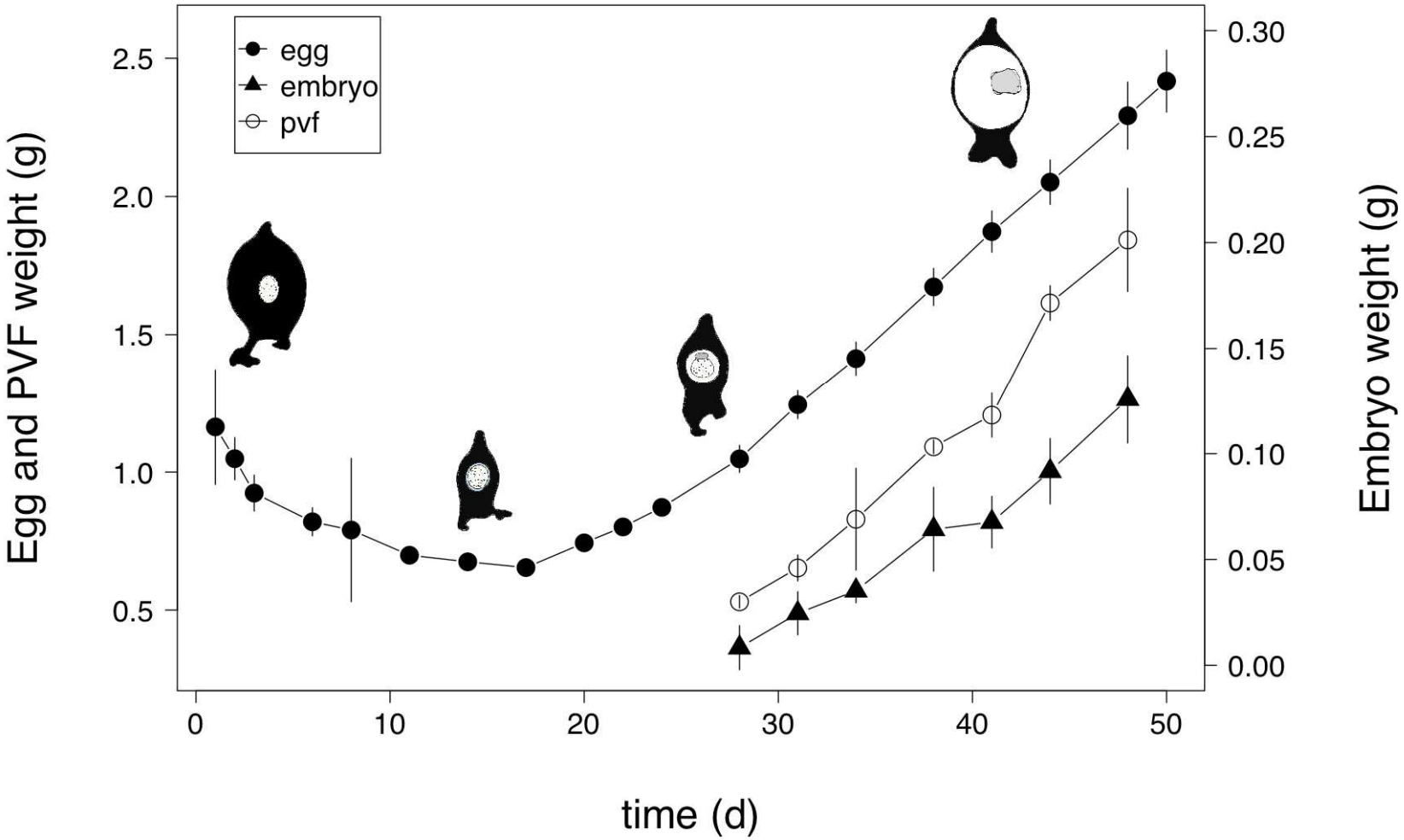
egg
embryo
pvf
Egg and PVF weight (g)
Embryo weight (g)
time (d)
0.5
1.0
1.5
2.0
2.5
0.00
0.05
0.10
0.15
0.20
0.25
0.30
0
10
20
30
40
50

Figure 2

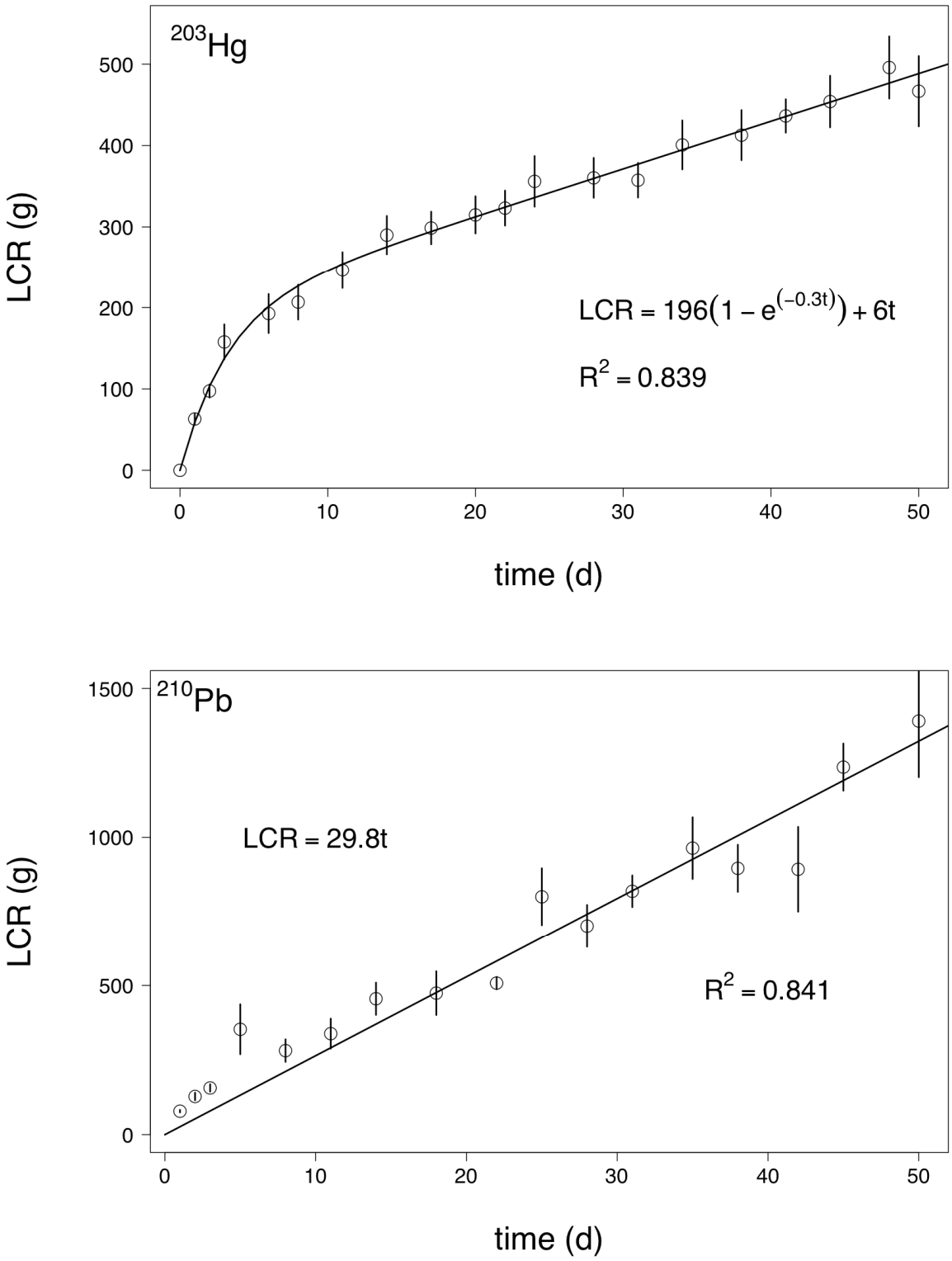
203Hg
LCR (g)
time (d)
LCR = 196(1 – e(–0.3t)) + 6t
R2 = 0.839
0
100
200
300
400
500
0
10
20
30
40
50
210Pb
LCR (g)
time (d)
LCR = 29.8t
R2 = 0.841
0
500
1000
1500
0
10
20
30
40
50

Figure 3

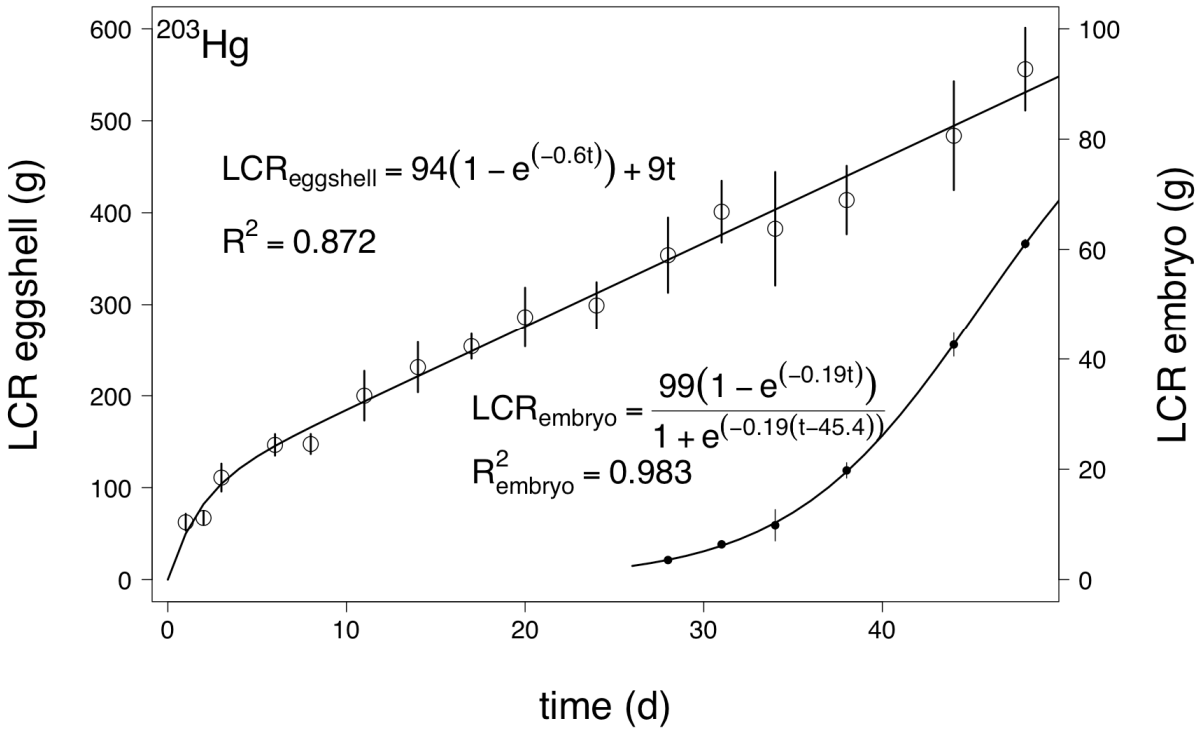
203Hg
LCR_eggshell = 94(1 − e^(−0.6t)) + 9t
R^2 = 0.872
LCR_embryo = 99(1 − e^(−0.19t)) / (1 + e^(−0.19(t−45.4)))
R^2_embryo = 0.983
LCR eggshell (g)
LCR embryo (g)
time (d)

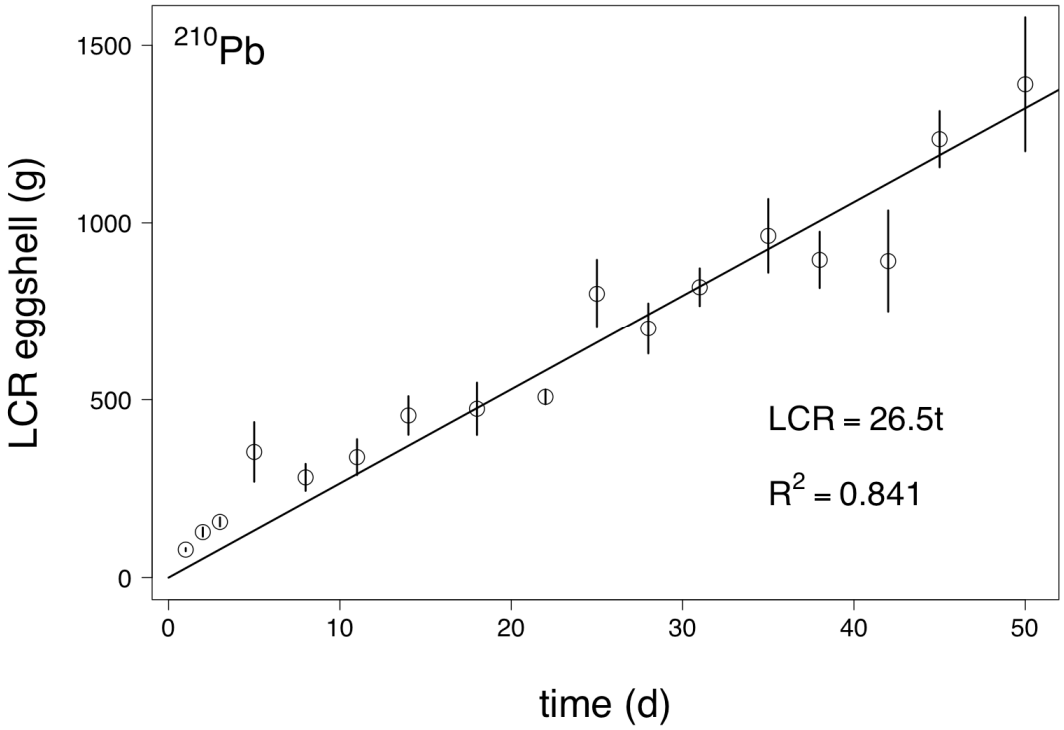
210Pb
LCR = 26.5t
R^2 = 0.841
LCR eggshell (g)
time (d)

Figure 4

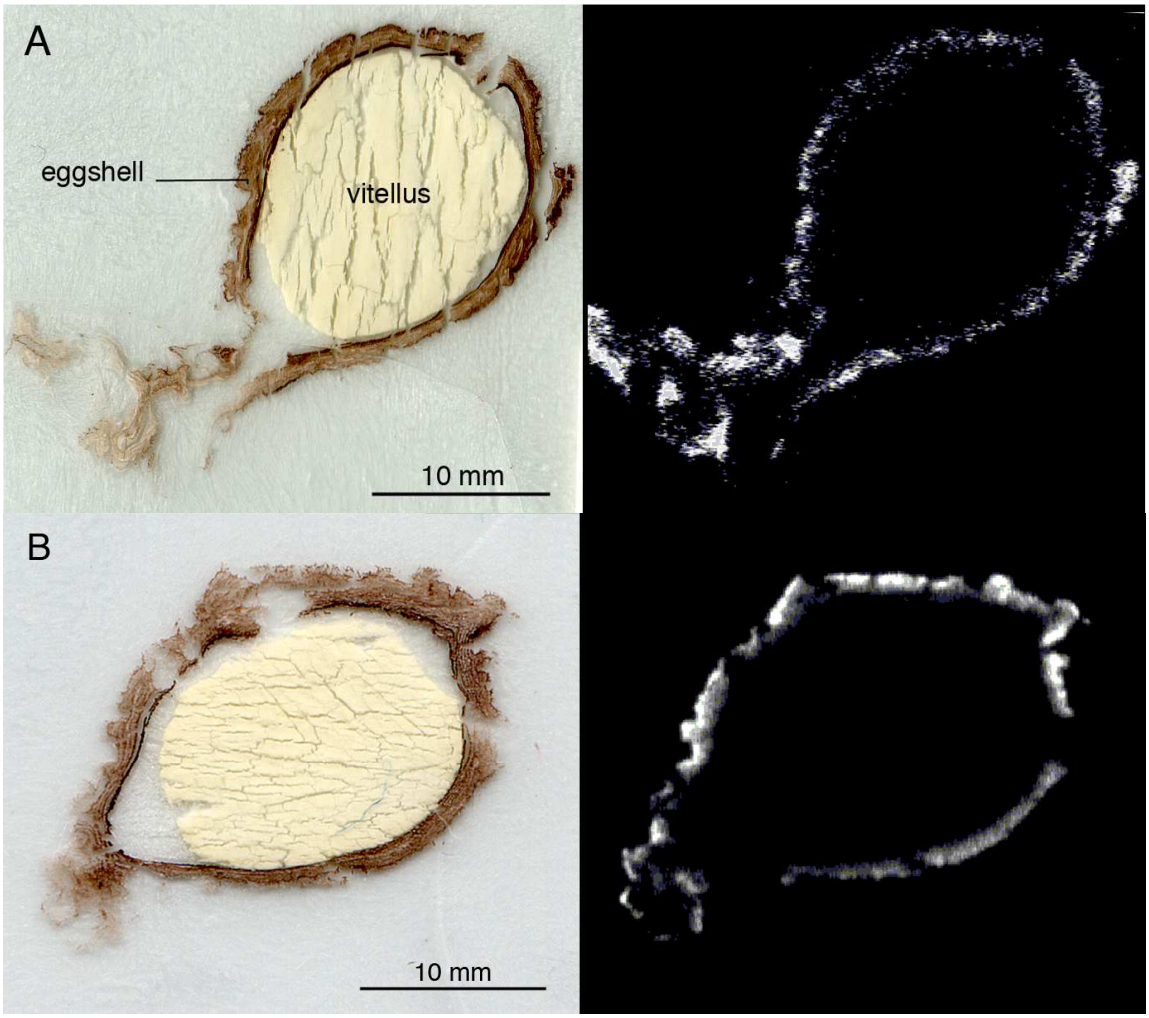

Figure 5